Consideration of microstructure in modelling the hydro-mechanical behaviour of unsaturated soils

Tianchi Wu[1], *Peter* Cleall[2, *], *Snehasis* Tripathy[3], and *Guoqing* Cai[4]

[1]Ph.D. student, School of Engineering, Cardiff University, Cardiff, United Kingdom

[2]Professor, School of Engineering, Cardiff University, Cardiff, United Kingdom.

[3]Professor, School of Engineering, Cardiff University, Cardiff, United Kingdom.

[4]Professor, School of Civil Engineering, Beijing Jiaotong University, Beijing, China.

Abstract. The hydro-mechanical behaviour of unsaturated soils is often highly influenced by the microstructure; therefore, it can be beneficial to consider the effect of microstructure in a hydro-mechanical constitutive model. This paper considers the use of a microstructure-related model that adopts the effective degree of saturation as a microstructural index. The model can be used to reproduce the hydro-mechanical behaviour while the effect of the microstructure is considered. For comparison, a non-microstructure-dependent model is also employed. The models are applied to simulate the behaviour of two different soils and a comparison of the models' performance in simulating triaxial test behaviour is made. Based on the comparison with experimental results and the non-microstructure-dependent model, it can be concluded that the adoption of the effective degree of saturation is beneficial to studying the hydro-mechanical behaviour of unsaturated soils affected by the microstructure.

1 Introduction

It is widely acknowledged that the microstructure is a key factor in accounting for the hydro-mechanical behaviour of the unsaturated soils. However, the relationship between the microstructure and the behaviour of soils still has not been fully studied due to the complexity and variability of the microstructure. Therefore, it is of value to describe the microstructure qualitatively and quantitively and investigate the effect of the microstructure on the hydro-mechanical behaviour of unsaturated soils.

Various methods have been proposed in the literature to describe the microstructure of soils. To study the permeability of the soils, more attention has been paid to the geometrical properties of the microstructure, such as the geometrical shapes, dimensions, and sizes ([1–4]). In terms of strength and deformation features, pore sizes, pore size distributions and intermolecular interaction are most widely adopted to describe the microstructure ([5–10]). Scanning Electrion Microscope (SEM) and Computed Tomography (CT) are popular methods to directly obtain images showing the microstructure and its evolution under loading ([10–17]).

A number of experimental investigations have been carried out to study the relationship between the microstructure and the hydro-mechanical behaviour of unsaturated soils. Based on results from consolidated undrained (CU) triaxial tests, mercury intrusion porosimetry (MIP) tests and SEM tests on a loess, Wang et al. ([18]) have reported that the particle morphology becomes less angular with the increase of confining stresses and that is consistent to the phenomena that the soil samples have more dense and homogenous deformation under a higher confining stress. Studies in the past have shown that soils with double porosity tend to have a bimodal water retention curve ([19–22]). Griffiths and Joshi ([23]) studied the consolidation stress-induced pore size evolution of a clay and concluded that inter-aggregate pores are the main source of the volume change while the intra-aggregate pores remain almost unaffected during consolidation. Theoretical models have also been established to consider the effect of the microstructure on the behaviour of soils. Zou ([1]) considered the geometrical properties of the microstructure and has proposed a macroscopic model for predicting the relative hydraulic permeability of unsaturated soils. To study the stress-strain behaviour of soils with double porosity, Sanchez et al. ([24]) considered both the macrostructural and microstructural levels and proposed a model to predict the mechanical behaviour of each level and the interaction between these two levels. Recently, Wu et al.

---

* Corresponding author: cleall@cardiff.ac.uk

([25]) have reported a microstructure-related model. The model was validated by considering various soil types under different loading conditions. The model was established based on the framework of the Glasgow Coupled Model (GCM) ([26,27]). Instead of using the degree of saturation to calculate the effective stress as in the case of GCM, the microstructure-related model by Wu et al. [26] adopted the effective degree of saturation as an indicator of the microstructure. The effective degree of saturation eliminates the influence of the microscopic degree of saturation which is related to the disconnected water within intra-aggregate pores and has no contribution to the effective stress ([28]). The model is thus able to consider the impact of the microstructure on the stress-strain behaviour of unsaturated soils.

The current study investigates the performances of the microstructure-related model established by Wu et al. ([25]) and the non-microstructure-related model (GCM). The experimental results of two soils are considered to evaluate the performances of the models.

2 Formulation of a microstructure related model

The establishment of the new model presented in ([25]), which considers the microstructure, is based on the widely used Glasgow Coupled Model (GCM) ([25–27]). The non-microstructure-dependent GCM has been modified to develop a microstructure-related model by replacing the degree of saturation by the effective degree of saturation. The effective degree of saturation is considered to be microstructure related because this index discards the effect of the microscopic degree of saturation which derives from the water within intra-aggregate pores ([28]) and contributes little to the Bishop's effective stress ([29]). The effective degree of saturation is defined as:

$$S_e = (S_r - S_r^m)/(1 - S_r^m) \qquad (1)$$

where S_r is the degree of saturation; S_r^m is the microscopic degree of saturation. The effective stress tensor is then defined as:

$$\sigma_{ij}^* = \sigma_{ij} - (S_e u_w + (1 - S_e)u_a)\delta_{ij} \qquad (2)$$

where σ_{ij} is the total stress tensor; u_w is the water pressure; u_a is the air pressure; δ_{ij} is the Kronecker delta. The basic framework of the microstructure-related model is defined below ([25–27]).

Yield surfaces:

$$F_{LC} = q^2 - M^2 p^*(p_0^* - p^*) = 0 \qquad (3)$$
$$F_{SD} = s_D^* - s^* = 0 \qquad (4)$$
$$F_{SI} = s^* - s_I^* = 0 \qquad (5)$$

Coupling among Yield surfaces:

$$ds_I^*/s_I^* = ds_D^*/s_D^* = k_2 dp_0^*/p_0^* \quad \text{(Yield on LC)} \qquad (6)$$
$$dp_0^*/p_0^* = k_1 ds_I^*/s_I^* = k_1 ds_D^*/s_D^* \quad \text{(Yield on SD/SI)} \qquad (7)$$

Flow rules:

$$d\tilde{\varepsilon}_j^p = d\lambda_l^j \frac{\partial F_l}{\partial \tilde{\sigma}^*} \quad \text{with} \quad \begin{array}{l} l = LC, \beta; j = LC, \beta, LC + \beta; \\ \beta = SI \quad \text{or} \quad SD \end{array}$$
$$(8)$$

Hardening laws:

$$dp_o^* = p_0^* \left[\frac{vd\varepsilon_v^p}{\lambda - \kappa} - \frac{k_1 dS_r^p}{\lambda_s - \kappa_s} \right]$$
$$(9)$$

$$ds_{I/D}^* = s_{I/D}^* \left[-\frac{dS_r^p}{\lambda_s - \kappa_s} + k_2 \frac{vd\varepsilon_v^p}{\lambda - \kappa} \right]$$
$$(10)$$

Constitutive relationship:

$$d\tilde{\sigma}^* = \boldsymbol{D}_e^* d\tilde{\boldsymbol{\varepsilon}}^e \quad \text{(elastic)} \qquad (11)$$
$$d\tilde{\sigma}^* = \boldsymbol{D}_e^* d\tilde{\boldsymbol{\varepsilon}}^e = \boldsymbol{D}_{ep}^* d\tilde{\boldsymbol{\varepsilon}} \quad \text{(elasto-plastic)} \qquad (12)$$

where p_0^* is the Bishop's pre-consolidation pressure which defines the position of F_{LC}; q is the deviator stress; p^* is the effective mean stress; s^* is the modifed suction; s_D^* and s_D^* are the modified suctions that locate F_{SI} and F_{SD}, respectively; k_1 and k_2 are coupling parameters; λ_s and κ_s are slopes for the normal consolidation line and rebound curve respectively; $d\varepsilon_v^p$ is the incremental plastic volumetric strain; dS_r^p is the incremental plastic degree of saturation; $d\lambda_l^j$ is the plastic multiplier with j related to the plastic mechanism which is active (e.g. when yield on LC yield surface is activated j is LC and for yield on SI or SD j is LC is β) and l is associated with plastic changes of effective degrees of saturation (when l is β) or volumetric strains (when l is LC); $d\tilde{\boldsymbol{\varepsilon}}^e$ is the incremental elastic strain vector , $d\tilde{\boldsymbol{\varepsilon}}$ is the incremental total strain vector and $d\tilde{\sigma}^*$ is the incremental effective stress vector; $\boldsymbol{D}_e^*$ is the generalized elastic matrix and $\boldsymbol{D}_{ep}^*$ is the generalized elasto-plastic matrix.

3 Model Application

The reported experimental results of two soils (Jossigny silt and a low-plastic clay) ([31,32]) were considered for studying the performances of the microstructure-related model and the GCM. The hydraulic and mechanical behaviour of the soils have been reported under different loading paths, namely wetting, drying, isotropic loading, shearing at various confining stresses and suctions. Some of these loading paths have been simulated by both the microstructure-related model and the GCM to obtain the stress-strain responses of the soils.

3.1 Jossigny silt

Jossigny silt is a non-expansive soil ([30]). Various isotropic compression and shear tests were conducted by Cui and Delage on unsaturated samples of the soil. The samples were prepared under the initial states shown in Table 1. The model parameters (see Table 2) were obtained based on the experimental results. The microscopic degree of saturation was derived based on the method suggested by Alonso ([28]). The soil samples first underwent a drying process to the targeted suctions.

Further, the samples were compressed to predetermined net mean stresses and sheared until failure.

Table 1. Initial states for the Jossigny silt samples

Initial states	Value
$\overline{p}/\text{kPa}$	25.00
s/kPa	200.00
e	0.629
S_r	76.4%
S_r^m	56.0%
p_0^*/kPa	374.60
S_D^*/kPa	77.23
S_I^*/kPa	103.84

Table 2. Model parameters for the Jossigny silt samples

| Parameters	Value
λ	0.091
κ	0.013
λ_s	0.131
κ_s	0.008
k_1	0.65
k_2	0.66
M	1.23
μ	0.3
G_s	2.78

Figure 1 presents the experimental axial strain versus deviator stress results during the shearing process conducted at constant suction of 200kPa and at constant confining stresses of 50kPa, 200kPa and 600kPa. Figure 2 presents the change in void ratio with the axial strain in the same tests. The simulation results are also shown in Figs. 1 and 2.

For the soil samples tested, the deviator stress increased and reached a maximum value at an axial strain of greater than 10%. It can be observed that samples sheared at a higher confining stress had a higher peak deviator stress, which is as expected, means that the shear strength increases with an increasing confining stress. Both the micro-related and non-micro-related models performed well in simulating the tendency of deviator stress change during shearing. However, both the models underestimated the deviator stress at all axial strains. This is a common issue that originates from the deficiency of the Modified Cam-Clay Model ([25,27]) upon which both the models are based.

During the early stage of shearing where the axial strain is smaller than 4%, the results from the micro-related model seem to be more consistent to the experimental results than the results from the non-micro-related model. However, the micro-related model significantly overestimated the axial strains when the stress path approached failure.

In terms of the void ratio, both the models successfully reproduced the trend of decreasing void ratio during shearing (see Fig. 2). The micro-related model demonstrates better consistency with the experimental results than the non-micro-related model. The latter tended to yield a higher volume change during shearing. This is because under the same loading condition, the effective stress is much larger in the non-micro-related model due to the fact that the microscopic degree of

saturation, which barely contributes to the effective stress, is incorporated into the Bishop's effective stress parameter. When the stress path yields on both the LC and SD yield surfaces and generates large irreversible volumetric strains, the difference in the effective stresses calculated by these two different models will further amplify the disparity in the void ratio change. In Fig. 2 the starting point of the simulation results are different from the experimental void ratios because both the models use the results of simulated isotropic compression to define the initial state.
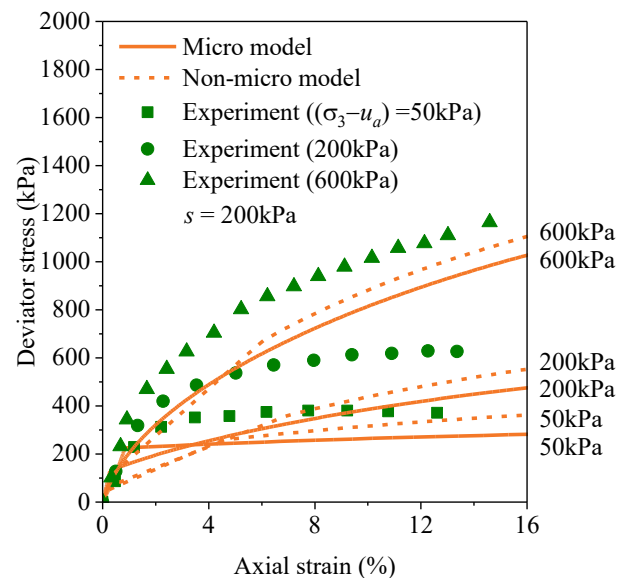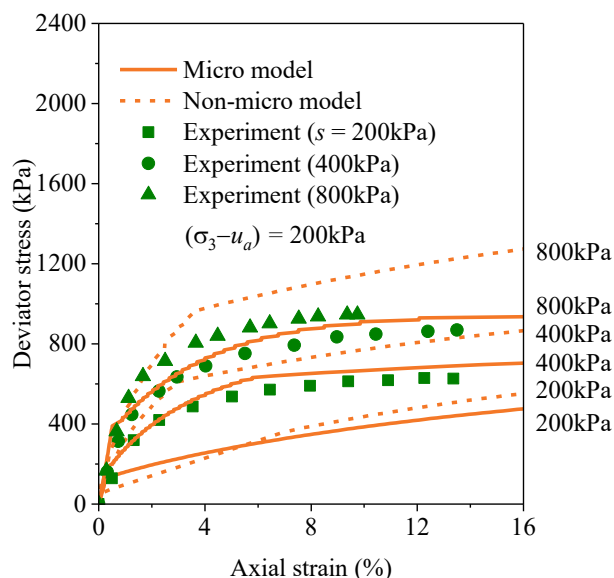

Fig. 1. Comparison of model and experimental results in terms of deviator stress for Jossigny silt ([30]) at s = 200kPa.
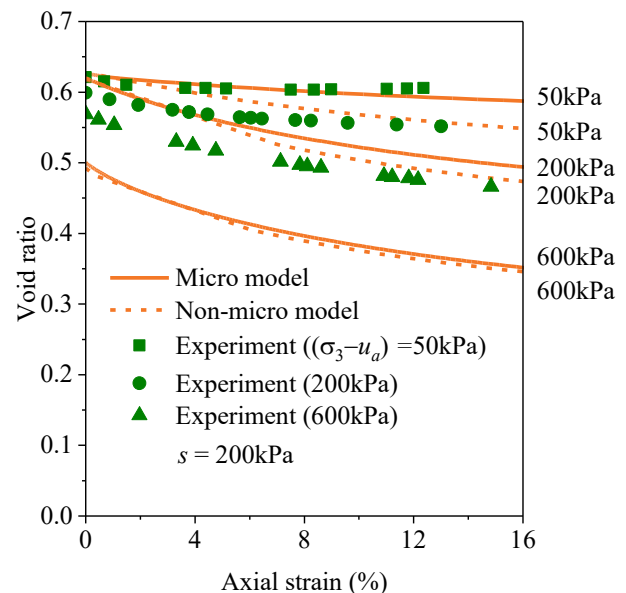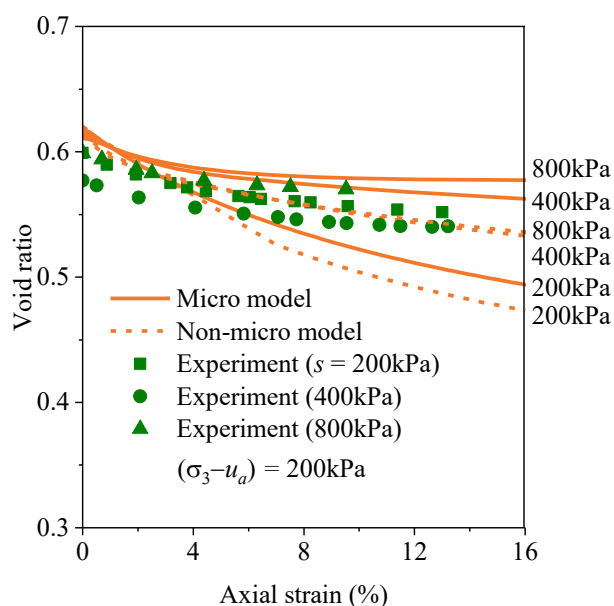

Fig. 2. Comparison of model and experimental results in terms of void ratio for Josisigny silt ([30]) at s = 200kPa.

Fig. **3** shows how the deviator stress changes during shearing at the same confining stress but at different suctions of 200kPa, 400kPa and 800kPa. Figure 4 presents

the change in void ratio in the same tests. Both the models still have a satisfactory performance in simulating the deviator stress change and the void ratio change. When the samples were sheared at suctions of 200 and 400kPa, both the models overestimated the development of axial strain and the non-micro-related model produced results closer to the experimental results. When modelling shear at a constant suction of 800kPa, the non-micro-related model significantly overestimated the shear strength while the micro-related model produced a more reasonable output.

Fig. 3. Comparison of model and experimental results for Jossigny silt ([30]) at various suctions and $(\sigma_3 - u_a) = 200$kPa.

Fig. 4. Comparison of void ratio between model and experimental results ([30]) at various suctions and $(\sigma_3 - u_a) = 200$kPa.

The micro-related model performed better than the non-micro-related model in terms of the void ratio (see Fig. 4). The micro-related model slightly underestimated the void ratio change while the non-micro-related model overestimated the void ratio change at the suction of 400 and 800kPa. Both the micro-related model and the non-micro-related model overestimated the void ratio change when the suction was 200kPa, but the micro-related model produced a closer simulation of the experimental results.

Since both the models were found to overestimate the axial strain to reach the critical state in most cases, the 20% axial strain was adopted as a reference strain for the critical state of the modelling results. Table 3 shows the results of the simulated degree of saturation values at this specific axial strain and the experimental results at various suctions and confining stresses. It can be noticed that the micro-model was not necessarily better than the non-micro-related model in predicting the degree of saturation. The adoption of the effective degree of saturation is an oversimplified way to consider the microstructure and more investigations are needed to describe the microstructure more effectively.

Table 3. Comparison of experimental and model results in terms of degree of saturation for Jossigny silt at confining stress of 50,200 and 600kPa and at constant suctions of 200, 400 and 800kPa.

s /kPa	σ_3 /kPa	S_r /%(micro)	S_r /%(non-micro)	S_r /%(experiments)
200	600	90.9	100	98.0
200	200	83.3	95.2	79.0
200	50	78.4	86.2	79.0
400	200	75.1	77.6	77.0
800	200	70.0	67.4	70.0

3.2 Low-plastic clay

A low-plastic clay used by Almahbobi ([31]) was a mixture of 40% Leighton Buzzard sand, 40% M400 silt and 20% Speswhite kaolin. The compacted soil samples were initially at a suction of 563kPa and degree of saturation of 36.2%. The samples were wetted to targeted suction of 300kPa at a constant confining stress of 20kPa. The samples were then compressed to predetermined confining stresses of 100, 250, 400kPa before shearing. The initial states and the model parameters of the samples are shown in Table 4 and Table 5 respectively.

**Table 4.** Initial states for the low-plastic clay.

Initial states	Value
$\overline{p}$/kPa	20.00
s/kPa	563.00
e	0.732
S_r	36.2%
S_r^m	10.0%
p_0^*/kPa	250.00
S_D^*/ kPa	237.94
S_I^*/ kPa	/

Table 5. Model parameters for the low-plastic clay.

Parameters	Value
λ	0.07
κ	0.008
λ_s	0.12
κ_s	0.02
k_1	0.6
k_2	0.3
M	1.076
μ	0.3
G_s	2.65

Figure 5 presents the experimental axial strain versus deviator stress results during the shearing process conducted at constant suction of 300kPa and at constant confining stresses of 100kPa, 250kPa and 400kPa. Figure 6 presents the change in void ratio with the axial strain in the same tests. The simulation results are also shown in Figs. 5 and 6.

As shown in Fig. 5, the micro-related model performed better in simulating the increasing deviator stress during shearing while the non-micro-related model slightly overestimated the deviator stress at constant confining stresses of 250 and 400 kPa. This overestimation became more significant at the confining stress of 100kPa. Correspondingly, while the micro-related model produced results that are closer to the experimental results, the difference between the micro-related model and the non-micro-related model narrowed with the increase of the confining stress (see Fig. 6).
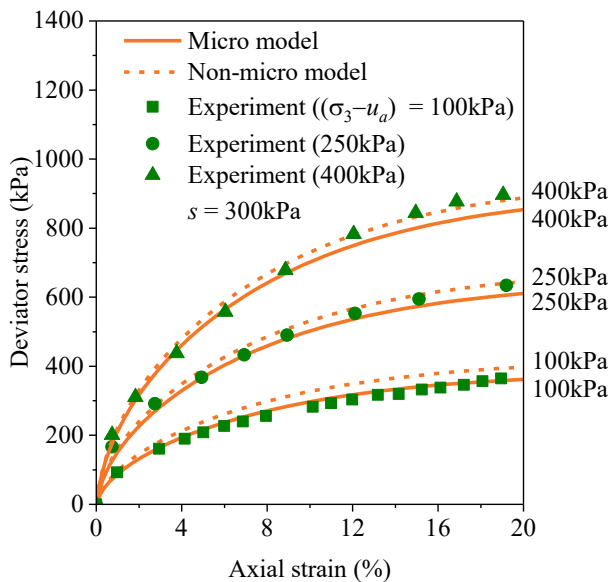
Fig. 5. Comparison of model and experimental results in terms of deviator stress for the low-plastic clay ([32]) at s = 300kPa.
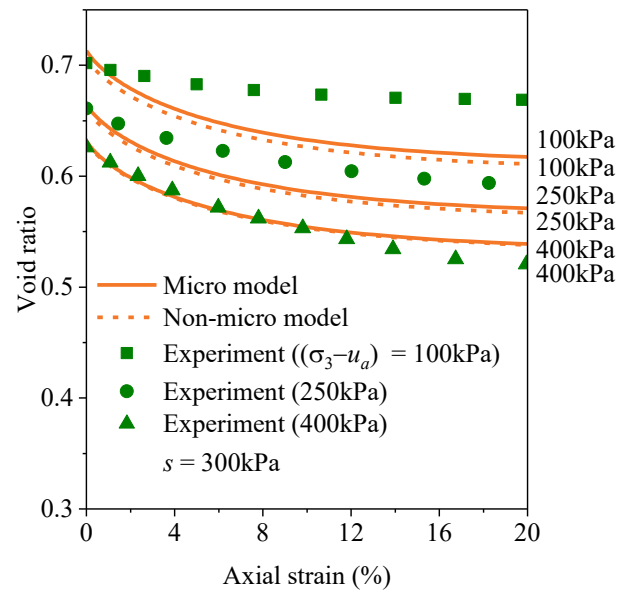
Fig. 6. Comparison of model and experimental results in terms of void ratio for the low-plastic clay ([32]) at s = 300kPa.

4 Conclusions

This paper studies the importance of considering the effects of the microstructure on the hydro-mechanical behaviour of unsaturated soils. Two reported models including a microstructure-related model and a non-microstructure-related model were used to reproduce the behaviour of soils under different stress paths in triaxial tests. The microstructure-related model was established based on the Glasgow Coupled Model, but the effective stress was calculated considering the effective degree of saturation, a microstructure-related index, instead of the degree of saturation which is more widely used in many hydro-mechanical constitutive models. The simulated performance of the microstructure-related model has been validated by comparing it with the Glasgow Coupled Model (GCM) and the experimental results of Jossigny silt and a low-plastic clay.

The findings from the study suggested that the models can satisfactorily reproduce the mechanical behaviour of soils during shearing, but the microstructure-related model tends to produce a slightly better estimation of the void ratio change despite the fact that the difference can be narrowed between these two models at a higher confining stress or suction. When modelling the behaviour of Jossigny silt, both the models overestimated the axial strain to reach failure. The microstructure-related model performed better in predicting the void change, whereas the GCM overpredicted the volume change during shearing. In terms of modelling the behaviour of a low-plastic clay, the deviator stress at a specific axial strain, the shear strength and the void ratio change were overestimated by the GCM, whereas the results from the microstructure-related model were found to be in good agreement with the experimental results. The differences between the results from the two models became smaller at higher confining stresses.

The study suggested that it is beneficial to consider the effect of microstructure on the behaviour of unsaturated

soils by implementing the effective degree of saturation, which is a microstructural index, in a hydro-mechanical model. Due to the simplification of describing the microstructure through the effective degree of saturation, more efficient ways of considering the microstructure remain to be investigated to increase the performance of a microstructure-related model.

References

1. Y. Zou, Acta Geotech. **7**, 129 (2012)
2. W. F. Brace, J. Geophys. Res. 1896-1977 **82**, 3343 (1977)
3. Y. F. Liu, D.-S. Jeng, Adv. Water Resour. **129**, 232 (2019)
4. Y. F. Xu, D. A. Sun, Phys. Stat. Mech. Its Appl. **316**, 56 (2002)
5. A. Das, A. Kumar, Géotechnique Lett. **7**, 24 (2017)
6. Q.-F. Gao, M. Jrad, M. Hattab, J.-M. Fleureau, L. I. Ameur, Int. J. Geomech. **20**, 4020057 (2020)
7. J. Kan, G. Li, N. Zhang, P. Wang, C. Han, S. Wang, Geofluids **2021**, e6664925 (2021)
8. H. Tanaka, D. R. Shiwakoti, N. Omukai, F. Rito, J. Locat, M. Tanaka, Soils Found. **43**, 63 (2003)
9. T. V. Alekseeva, Eurasian Soil Sci. **40**, 649 (2007)
10. E. Romero, P. H. Simms, Geotech. Geol. Eng. **26**, 705 (2008)
11. Y. Chen, A. Banin, Soil Sci. **120**, 428 (1975)
12. Y. Chen, J. Tarchitzky, J. Brouwer, J. Morin, A. Banin, Soil Sci. **130**, 49 (1980)
13. O. Onofiok, M. J. Singer, Soil Sci. Soc. Am. J. **48**, 1137 (1984)
14. S. Crestana, R. Cesareo, S. Mascarenhas, Soil Sci. **142**, 56 (1986)
15. L. Luo, H. Lin, P. Halleck, Soil Sci. Soc. Am. J. **72**, 1058 (2008)
16. I. A. Taina, R. J. Heck, T. R. Elliot, Can. J. Soil Sci. **88**, 1 (2008)
17. J. K. Torrance, T. Elliot, R. Martin, R. J. Heck, Cold Reg. Sci. Technol. **53**, 75 (2008)
18. Y. Wang, H. Yang, X. Jing, Geotech. Geol. Eng. **39**, 65 (2021)
19. C. A. Burger, C. D. Shackelford, Can. Geotech. J. **38**, 53 (2001)
20. N. Romano, P. Nasta, G. Severino, J. W. Hopmans, Soil Sci. Soc. Am. J. **75**, 468 (2011)
21. A. Satyanaga, H. Rahardjo, E.-C. Leong, J.-Y. Wang, Comput. Geotech. **48**, 51 (2013)
22. H. Zhou, S. J. Mooney, X. Peng, Soil Sci. Soc. Am. J. **81**, 1270 (2017)
23. F. J. Griffiths, R. C. Joshi, Géotechnique **39**, 159 (1989)
24. M. Sánchez, A. Gens, L. do N. Guimarães, S. Olivella, Int. J. Numer. Anal. Methods Geomech. **29**, 751 (2005)
25. T. Wu, G. Cai, P. Cleall, S. Tripathy, Int. J. Geomech. **22**, 04022216 (2022)
26. S. J. Wheeler, R. S. Sharma, M. S. R. Buisson, Géotechnique **53**, 41 (2003)
27. M. Lloret-Cabot, M. Sánchez, S. J. Wheeler, Int. J. Numer. Anal. Methods Geomech. **37**, 3008 (2013)
28. E. E. Alonso, J.-M. Pereira, J. Vaunat, S. Olivella, Géotechnique **60**, 913 (2010)
29. A. W. Bishop, Tek. Ukebl. **39**, 859 (1959)
30. Y. J. Cui, P. Delage, Géotechnique **46**, 291 (1996)
31. S. A. Almahbobi, Experimental Study of Volume Change and Shear Strength Behaviour of Statically Compacted Collapsible Soil, Cardiff University, (2018)